DOI: 10.1002/chem.200500973

Investigation of Guanosine-Quartet Assemblies by Vibrational and Electronic Circular Dichroism Spectroscopy, a Novel Approach for Studying Supramolecular Entities

Vladimír Setnička,*[a] Marie Urbanová,[a] Karel Volka,[a] Sreenivasachary Nampally,[b] and Jean-Marie Lehn*[b]

Abstract: The self-assembly of guanosine-5′-hydrazide **G-1** in D_2O, in the presence and absence of sodium cations, has been investigated by chiroptical techniques: electronic (ECD) and the newly introduced vibrational (VCD) circular dichroism spectroscopy. Using a combination of ECD and VCD with other methods such as IR, electron microscopy, and electrospray ionization mass spectrometry (ESI-MS) it was found that **G-1** produces long-range chiral aggregates consisting of G-quartets, $(\mathbf{G\text{-}1})_4$, subsequently stacked into columns, $[(\mathbf{G\text{-}1})_4]_n$, induced by binding of metal cations between the $(\mathbf{G\text{-}1})_4$ species. This process, accompanied by gelation of the sample, is highly efficient in the presence of an excess of sodium cations, leading to aggregates with strong quartet–quartet interaction. Thermally induced conformational changes and conformational stability of guanosine-5′-hydrazide assemblies were studied by chiroptical techniques and the melting temperature of the hydrogels formed was obtained. The temperature-dependent experiments indicate that the long-range supramolecular aggregates are dissociated by increasing temperature into less ordered species, monomers, or other intermediates in equilibrium, as indicated by MS experiments.

Keywords: circular dichroism · guanosine · hydrogels · self-assembly · supramolecular chemistry

Introduction

Guanine (G) derivatives are important motifs not only in biology, but also in supramolecular chemistry and nanotechnology.[1–4] Indeed, they undergo self-recognition and self-assembly processes leading to complex supramolecular structures based on the formation of cyclic tetrameric entities, G-quartets, stabilized by metal-ion binding. Self-assembled G species have been characterized in crystals,[5–11] as well as in aqueous solutions[12–15] and organic media.[16–18] They represent a specially interesting class of systems within the framework of supramolecular self-organization.[19,20] A number of studies have focused on guanine-rich oligonucleotides that give rise to structures containing G-quartets and play an important biological role.[1,21–25] G-quartets are formed by G-rich telomeric DNA located at the end of eukaryotic chromosomes and are targets for inhibitors of telomerase activity of potential interest to cancer therapy.[26,27] In addition, G-rich repeats also occur in other parts of the human genome and, therefore, quartet formation may also be important for other diseases.[28]

We have recently reported that guanosine-5′-hydrazide **G-1** forms remarkably stable hydrogels in presence of metal ions and have investigated the sol–gel phase transition as a function of various physical and chemical parameters.[29] Guanosine **G-1** is in particular able to select side chain groups, dynamically attached through acylhydrazone formations, that generate the strongest gels.

We now describe a structural study of the assemblies formed by **G-1** based on circular dichroism (CD) chirospectroscopic methods.

The purine base guanine G itself is planar,[30] and thus is not optically active. In guanosine, G is attached to the 1′-carbon atom of the chiral ribose, which can induce a CD in the base chromophore bands in the UV/Vis region. Each base can be deformed slightly from its ideal monomer ge-

[a] Dr. V. Setnička, Prof. M. Urbanová, Prof. K. Volka
Institute of Chemical Technology, Technická 5
166 28 Prague 6 (Czech Republic)
Fax (+420) 224-310-352
E-mail: vladimir.setnicka@vscht.cz

[b] Dr. S. Nampally, Prof. J.-M. Lehn
ISIS, Université Louis Pasteur, CNRS UMR 7006
BP 70028, 67083 Strasbourg (France)
Fax: (+33) 390-245-140
E-mail: lehn@isis.u-strasbg.fr

ometry upon complex formation with appropriate metal cations. Therefore, the electronic circular dichroism spectroscopy (ECD)[31] can be easily and conventionally used to study the chirality changes of such guanosine-containing systems.[32,33] ECD spectroscopy is sensitive to the architecture of the assembled species for which exciton double-signed bands are often observed, corresponding to a single absorption band in the UV/Vis spectrum. However, the molecules need accessible transitions in UV/Vis region, which generally limit the ECD technique to chromophoric molecules, with a large coupling of the electronic transition dipoles in the molecule. Since these transitions are usually broad and overlapping, their individual frequencies do not provide much information on the correlation of ECD spectral properties with structural features. Therefore, the usual interpretations employ bandshape-based schemes that are either qualitative or dependent on a statistical fit to a set of spectra that provide the structural reference set.

While ECD spectroscopy in UV/Vis region has already been employed in the study of guanosine assemblies,[3,13,32] another chiroptical technique is presented here, vibrational circular dichroism spectroscopy (VCD),[34–37] as a new and promising technique to investigate the structure of these complex chiral self-assembled systems. In contrast to ECD, the VCD operating in IR region has the usual spectral advantages found in IR and Raman spectroscopy of a large number of resolved, relatively localized (corresponding to specific bond types) transitions, rather than the few, broad, overlapping vibronic bands found in the UV region. Therefore, the VCD spectra provide valuable information on the involvement of specific parts of molecules in the formation of chiral self-assemblies and sensitively reveal the parts of molecules the optical activity of which is influenced by supramolecular structure formation. Thus, VCD give structural information on chiral molecules that is not easily obtainable by other nonchiroptical techniques. Some of us have been developing VCD not only to study noncovalent interactions of biologically interesting molecules,[38–43] but also to extend its applicability to the field of supramolecular chemistry.[44–46]

Abstract in Czech: *Proces samoskladby guanosin-5′-hydrazidu **G-1** v D_2O roztocích, bez a za přítomnosti sodných iontů, byl studován chiroptickými metodami: spektroskopií elektronového (ECD) a nově také vibračního (VCD) cirkulárního dichroismu. Kombinací spektroskopie ECD a VCD s jinými metodami jako IČ spektroskopií, elektronovou mikroskopií a hmotnostní spektrometrií s ionizací elektrosprejem (ESI-MS) bylo zjištěno, že molekula **G-1** vytváří rozsáhlé chirální útvary složené z G-kvartetů, $(\mathbf{G\text{-}1})_4$, které mohou být následně za přítomnosti kationtů spojeny patrovými interakcemi za vzniku uspořádaných vláken, $[(\mathbf{G\text{-}1})_4]_n$. Tento proces spojený s gelovatěním vzorku je vysoce účinný v přítomnosti sodných kationtů, které vedou ke vzniku agregátů fixovaných silnými interakcemi mezi jednotlivými kvartety. Teplotně indukované konformační změny a konformační stabilita samoskladných útvarů tvořených guanosin-5′-hydrazidem byly studovány chiroptickými metodami a byly získány teploty tání připravených hydrogelů. Teplotně závislé experimenty ukázaly, že rozsáhlé supramolekulární útvary jsou se vzrůstající teplotou rozrušovány za vzniku útvarů méně uspřádaných, monomerů nebo některých intermediátů, které jsou ve vzájemné rovnováze, jak bylo indikováno MS experimenty.*

Experimental Section

Materials: Guanosine-5′-hydrazide (**G-1**) was synthesized and characterized as described previously.[29]

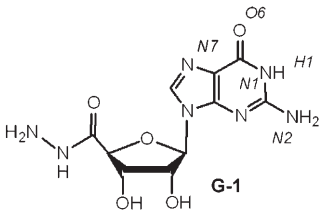

G-1

Deuterium oxide (D_2O, 99.9% D, Isosar) and [D_6]dimethylsulfoxide ([D_6]DMSO, 99.8% D, Isosar) were used as solvents. [D_3]Phosphoric acid (D_3PO_4, 99% D) and sodium hydroxide (NaOD, 99.5% D) were purchased from Aldrich and used for preparation of 0.5 mol L^{-1} deuterated sodium phosphate/D_2O buffer solution (pD = 6.1).

Methods: The samples for IR absorption and VCD measurements were prepared by mixing **G-1** at concentration range 3.0–12.0 g L^{-1} (~10–38 mmol L^{-1}) with sodium phosphate/D_2O buffer (0.5 mol L^{-1}; pD = 6.1). Because of low **G-1** solubility at room temperature, the mixture was heated until dissolution. The heating step was also useful to achieve equilibration of the H-D exchange between the sample and solvent. The solution was then cooled back to room temperature and the sample was placed in a demountable cell A 145 (Bruker, Germany) composed of two CaF_2 windows separated by a 25 μm Teflon spacer. For temperature-dependent IR and VCD experiments, a demountable electrically heated cell P/N20500 (Specac, UK) constructed of CaF_2 windows separated by a 25 μm Teflon spacer and equipped with the heated jacket controller 3000 Series (Specac, UK) was used. The temperature range studied was 20–90 °C in steps of 10 °C.

When [D_6]DMSO used as a solvent, the IR and VCD experiments were performed by using a 100 μm Teflon spacer and a **G-1** concentration of 17.0 g L^{-1} (~55 mmol L^{-1}).

For both cells used for IR and VCD experiments, the sample was introduced by filling holes in case of solutions (sol phase). For **G-1** in a gel phase, the gel was heated up until melting and the sol obtained was subsequently placed on the CaF_2 window, then covered by the second window separated by a 25 μm spacer. Finally, the cell was assembled into the steel cell holder and VCD spectra recorded when the sample had cooled down and was fully gelated. Spectral homogeneity of the samples inside the cells was checked by obtaining the same IR and VCD patterns for various cell positions. In addition, the hydrogels were prepared a few times giving very good VCD spectra reproducibility.

The IR and VCD spectra were recorded by using a FT-IR spectrometer IFS-66/S equipped with the VCD/IRRAS module PMA 37 (Bruker, Germany) by a procedure described elsewhere.[47] The VCD spectra were obtained as an average of six blocks of 3380 scans (each block accumulated for 30 minutes) at 4 cm^{-1} spectral resolution and processed with a zero-filling factor of 4. The vibrational spectra presented were expressed in molar absorptivity ε (L mol^{-1} cm^{-1}) per one **G-1** molecule. The quality of

the VCD measurements was demonstrated by typical noise spectra that were calculated as a standard deviation of all the six blocks of VCD scans.

The ECD spectra were measured on a Jasco J-810 spectropolarimeter (Japan) equipped with a thermostatted cell holder attached to a Jasco Peltier temperature control system PTC-423S with an accuracy of the temperature setting of 0.2 °C. The ECD spectra of samples at concentrations from ~20 mmol L^{-1} to 40 μmol L^{-1} were measured in 0.5 mol L^{-1} sodium phosphate/D_2O buffer (pD = 6.1) as well as in pure D_2O for the temperature range from 10 to 90 °C in 10 °C steps. ECD spectra were recorded using 0.1, 1, and 10 mm quartz cells over the 180–350 nm wavelength region as an average of four scans measured with 1 nm bandwidth, 1 s response and 100 nm min^{-1} scanning speed. All the IR, VCD, and ECD spectra of the samples were baseline-subtracted by using a spectrum of the solvent obtained in the same experimental conditions.

Molecular modeling: Molecular modeling and energy minimization were performed using the semiempirical PM3 method and by using molecular mechanics MM+ method provided in the commercially available HyperChem 5.0 package (Hypercube, Inc., Waterloo, Ontario, Canada). The geometry of **G-1** was first calculated for the monomeric form and then the geometry of the $(\mathbf{G\text{-}1})_4$ quartet, involving sodium cations, was optimized based on the structure of the **G-1** monomer, both using semiempirical PM3 method. Then, the energy minimized structure of two stacked quartets, $[(\mathbf{G\text{-}1})_4]_2$, was obtained using the molecular mechanics MM+ force field. All geometry optimizations and energy minimizations were performed with the Polak–Ribiere algorithm, using an RMS gradient of 0.1 kcal A^{-1} mol^{-1}, on PC Intel Pentium 4, CPU 2.60 GHz.

Results and Discussion

Solubility: While **G-1** was soluble in [D_6]DMSO, forming transparent colorless solutions and easily achieving a high (~20 g L^{-1}; ~64 mmol L^{-1}) concentration convenient for reliable IR and VCD analysis, the low solubility in pure D_2O did not allow us to perform reliable VCD experiments.

Much better solubility of **G-1** was reached in sodium phosphate/D_2O buffer relative to pure D_2O.[29] Guanosine **G-1** was mixed with an appropriate volume of buffer to achieve the concentration desired for the VCD measurements and the solution was heated up until the compound dissolved. In this way, samples with concentrations up to ~15 g L^{-1} (~48 mmol L^{-1}) could be obtained, sufficiently high for VCD measurements. Such samples generated hydrogels after cooling back to room temperature,[29] as **G-1** forms organized assemblies in presence of sodium cations. Finally, the sol phase was observed in sodium phosphate buffer for concentrations of **G-1** lower than ~3 g L^{-1} (~10 mmol L^{-1}). Close to this concentration, the sol phase became a more viscous sol that changed into a compact hydrogel phase at concentrations around ~6 g L^{-1} (~20 mmol L^{-1}) and higher.

IR and VCD spectroscopy: The IR and VCD spectra measured for solutions of **G-1** [D_6]DMSO and sodium phosphate/D_2O buffer at 55 and 10 mmol L^{-1} concentration, respectively, as well as the spectra of the hydrogel (38 mmol L^{-1}) prepared in sodium phosphate/D_2O buffer, are shown in the mid-IR spectral region in Figure 1. All the spectra presented were collected at room temperature. The samples give substantially different IR and especially VCD

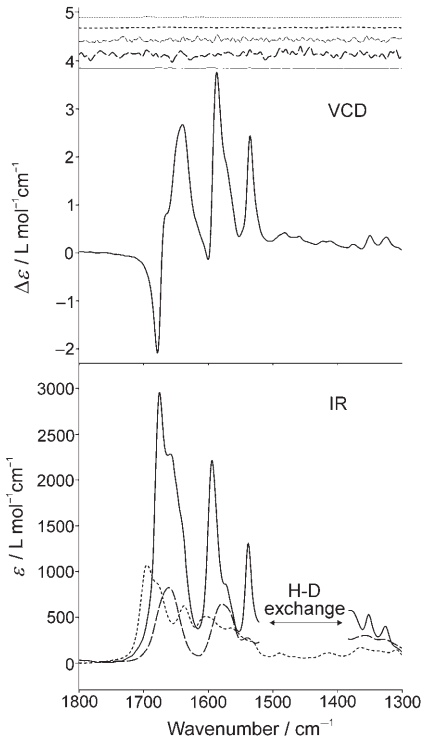

Figure 1. IR, VCD (both bold lines) and VCD noise (thin lines) spectra of **G-1** in [D_6]DMSO (dotted line, 55 mmol L^{-1}) and deuterated sodium phosphate/D_2O buffer at 10 and 38 mmol L^{-1} (dashed and solid lines, respectively). The 1400–1500 cm^{-1} region in the latter spectra is deleted for clarity. Concentrations were calculated per monomeric **G-1**.

spectra in the two solvents. While the ν(C=O) absorption maximum of **G-1** occurs at 1695 cm^{-1} in [D_6]DMSO, it is shifted to 1676 and 1661 cm^{-1} in sodium phosphate/D_2O buffer at concentrations of 38 and 10 mmol L^{-1}, respectively. The difference in ν(C=O) band positions is explained by the different species of **G-1** in the sample: The high ν(C=O) frequency in [D_6]DMSO (band at 1695 cm^{-1}) suggests that the C=O groups of **G-1** are present in a monomeric non-hydrogen bonded form, owing to the hydrogen-bond accepting character of [D_6]DMSO, which causes the disruption of intermolecular hydrogen bonds and therefore self-organization of **G-1** is prevented. The presence of the monomeric species of **G-1** in [D_6]DMSO is also supported by the absence of a VCD signal as there is no coupling of C=O modes among the isolated monomers. On the other hand, the shift of the ν(C=O) frequency to 1676 and 1661 cm^{-1} in sodium phosphate/D_2O buffer agrees with the participation of C=O groups in hydrogen bonding, either with D_2O or adjacent **G-1** molecule. Thus, the **G-1** molecules can be connected to each other creating a supramolecular network.[29]

The other absorption bands of **G-1** at ~1590 and ~1540 cm^{-1} are assigned to the δ(N–H) vibration of the NH_2 group (N2 nitrogen atom, see the diagram in the Experimental Section) mixed with aromatic ν(C=C) and ν(C=N) vibrations of the guanine moiety.[24,48] Both these bands, markedly seen for hydrogel at 38 mmol L^{-1}, were found to undergo intensity increase when the G residues were pres-

ent in highly ordered structures, for example, helices,[24] and provided sensitive probes of the existence of such structures. In the region between 1500–1400 cm^{-1}, the broad IR band centered at 1461 cm^{-1} results from H-D exchange of the sample in D_2O. This region is deleted for clarity in Figure 1.

While **G-1** has no significant VCD when dissolved in [D_6]DMSO (Figure 1), due to a monomeric form, a weak chirality enhancement was observed at 10 mmol L^{-1} in phosphate buffer owing to the presence of hydrogen bonded species. The VCD spectrum of the hydrogel at 38 mmol L^{-1} shows intense ν(C=O) VCD bands at 1679 cm^{-1} (−), 1641 cm^{-1} (+), and a shoulder at 1667 cm^{-1} (+), and is about 15 times larger than that of a 10 mmol L^{-1} solution. The positive couplet (bisignate VCD pattern, positive to lower and negative to higher energy) formed by these bands is slightly distorted from an ideal shape due to the contribution from the two types of carbonyl groups, that is, of the hydrazide and the guanine moieties (see diagram in the Experimental Section). These carbonyls give also two pronounced partly overlapping IR bands at 1676 and 1657 cm^{-1} in absorption spectrum. The other intense VCD bands at 1588 cm^{-1} (+) and 1536 cm^{-1} (+) are assigned, by comparison to IR absorption bands observed at these wavenumbers, to the δ(N-H) overlapping aromatic ν(C=C) and ν(C=N) vibrations. In the region below these bands, there are no significant VCD signals corresponding to a broad IR band arising from H–D exchange. The noise VCD spectrum calculated from the spectra measured at 38 mmol L^{-1} concentration shows a high S/N ratio and good stability of the gelated sample during the measurement at room temperature.

Taken together, the strong magnification in VCD intensity observed for the hydrogel at 38 mmol L^{-1} (Figure 1) is due to a coupling of C=O modes between particular molecules during the gelation process and may be attributed, according to similarity with published data,[44–46] to the formation of highly ordered supramolecular assemblies. Transmission electron microscopy revealed the presence of long fibers forming the gel.[29] The same results were obtained by atomic force microscopy (N. Sreenivasachary and J.-M. Lehn, unpublished data). Therefore, in agreement with the known behavior of guanine derivatives,[1,2] the present results and the previous study[29] show that **G-1** forms quartets $(\mathbf{G\text{-}1})_4$, as well as long-range aggregates consisting of G-quartets stacked into columns, $[(\mathbf{G\text{-}1})_4]_n$, induced by binding of metal cations between the $(\mathbf{G\text{-}1})_4$ species at 38 mmol L^{-1}. Such intense VCD signal of the hydrogel at this concentration implies that G-quartet units are probably not stacked in register, but are rotated with respect to one another to give a helical structure that could induce strong VCD signals as observed in Figure 1. The helical arrangement was also indicated, in accordance with literature,[24] by the bands at ~1590 and ~1540 cm^{-1} in the IR absorption spectrum. Although the shape of the VCD pattern in the ν(C=O) region (i.e., a positive couplet) is similar to that of molecules with a high guanosine content (poly(dG-dC)[49–51] and B-form DNA[49,52,53]) and forming a right-handed helical structure, the handedness of the stack is not clearly seen from the spectra. Nevertheless, we assume that $[(\mathbf{G\text{-}1})_4]_n$ could be right-handed, because the left-handed structures do not generally lead to a positive couplet in the ν(C=O) region but rather a negative one.[50] We have started ab initio DFT calculations of IR and VCD spectra for particular species to analyze the structural information provided by the spectroscopic data, especially whether the quartet formation can induce such a VCD pattern, or if it is possible to stack the quartets and calculate then the spectra.

By considering the single quartet $(\mathbf{G\text{-}1})_4$, complex formation with sodium cation has a significant influence on the electron distribution of G as reported for G-quartets.[54] An increase of the negative charges at O6 from −0.50 in isolated G, to −0.55 in a G-quartet and to −0.61 in a G-quartet with sodium cations[54] corresponds to complex formation with metal ions at O6/N7. Also, the positive charge increases at the hydrogen atoms involved in hydrogen bonds (H1 and two hydrogens at N2). The charge at O6 changes significantly when a sodium cation is located in the central cavity of the quartet, while the presence of the ion has less influence on H1, H at N2, and N7. It was also shown[54] that the acceptor atom, N3, is the most negative in the G-quartet. In addition, the negative electrostatic potential existing at the centers above and below the planes of a single quartet, together with the appropriate size of the central cavity, cause the sodium cation to bind inside the cavity,[8,12,14,55,56] close to the G-quartet plane. Such charge changes in the vicinity of the guanine carbonyl group may of course influence the ν(C=O) frequency when self-assembly takes place.

To gain more insight into the geometry of the species formed, structural modeling was performed by using semiempirical and molecular mechanics methods. The geometry of **G-1** and of the $(\mathbf{G\text{-}1})_4$ quartet with Na^+ was optimized. Subsequently, the initial geometry of two stacked quartets involving sodium cations, $[(\mathbf{G\text{-}1})_4]_2$, was obtained by combination of our geometries with structural data already published on similar molecules.[6,8,9,33] We also took into account the results of several theoretical studies of G-quartets that have been performed previously.[55,56] The complex was then energy minimized by using the MM+ method. Energy minimized structures of the quartet $(\mathbf{G\text{-}1})_4$ and of a double quartet stack $[(\mathbf{G\text{-}1})_4]_2$ are presented in Figure 2. Our molecular modeling results indicate that the guanine groups are slightly nonplanar as shown in the side view and, therefore, G-quartets show small deviations from the ideal coplanar C_{4h} symmetry and have nonplanar S_4-symmetric structures. These results are in very good agreement with those obtained by DFT ab initio calculations[54] suggesting that, for the isolated G-quartet, the form with S_4 symmetry is more stable than the planar C_{4h} form. The difference between these forms is, however, very small, about 0.4 kcal mol^{-1}.[54] The quartets are spaced at a distance of 3.3 Å and are rotated by ~30°, which allows the formation of a helical structure. Both these values are in agreement with the distances[8,9,14] and angles[1,6,57–60] experimentally found for G-quartet stacks. Therefore, the stacking of G-quartets may lead to

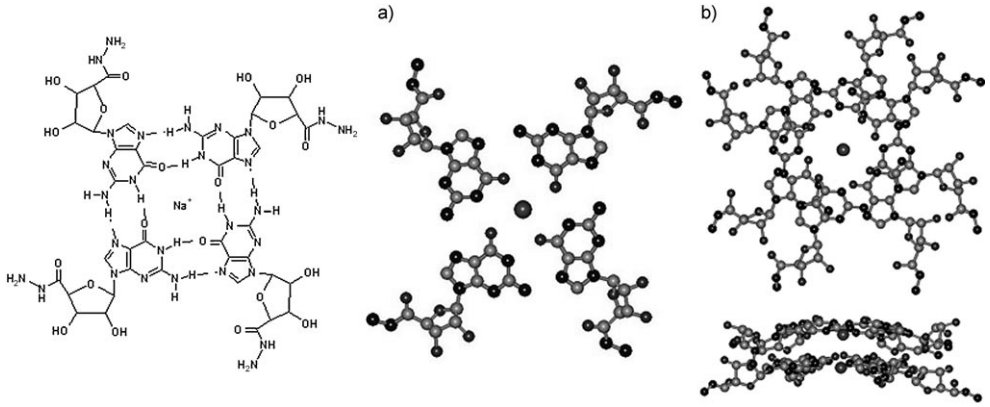

Figure 2. Energy minimized structure of a) $(\mathbf{G\text{-}1})_4$ quartet and b) its columnar stacking resulting into $[(\mathbf{G\text{-}1})_4]_n$ structure in top- and side-view arrangement of two stacked quartets $[(\mathbf{G\text{-}1})_4]_2$.

chirality propagation and is a reason for enhancement of VCD signals as observed for a gel phase in Figure 1.

To investigate the thermal stability of the hydrogel over a range of temperatures, the temperature-dependent IR absorption and VCD spectra of **G-1**, at 38 mmol L^{-1} concentration in sodium phosphate/D_2O buffer, were measured (Figure 3). At 20 °C, the sample is in a gel phase and all of the IR and VCD band shapes and frequencies are the same as observed in Figure 1. The band assignment was given already above. When the sample is gradually heated to 90 °C in steps of 10 °C, the ν(C=O) peak intensity changes and a gradual shift of the IR absorption maxima from 1676 to 1661 cm^{-1} is observed. Similar shifts to lower frequencies and a decrease in intensity were observed for δ(N−H) and aromatic ν(C=C) and ν(C=N) vibrations (the bands at ~1590 and ~1540 cm^{-1}) suggesting a dissociation of supramolecular structure.

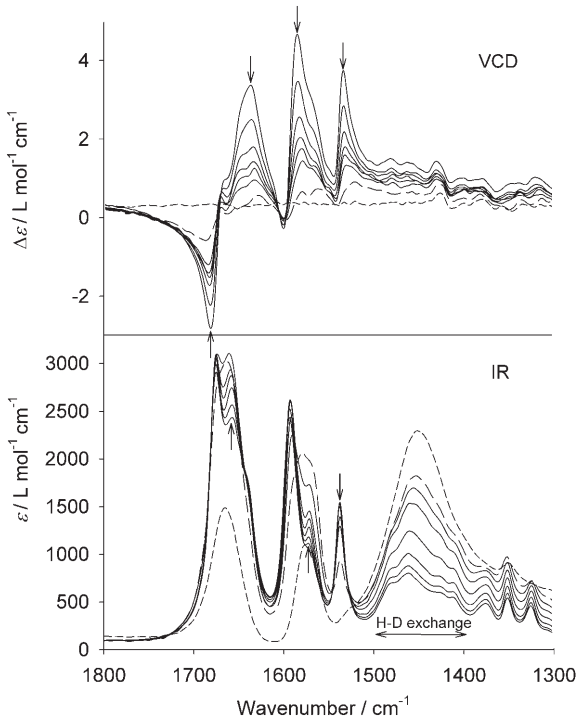

Figure 3. Gel melting experiments: IR and VCD spectra of **G-1** at 38 mmol L^{-1} concentration in 0.5 mol L^{-1} deuterated sodium phosphate/D_2O buffer. Spectra were measured from 20 °C to 90 °C in 10 °C increments. Spectra at 80 °C and 90 °C are plotted in long and short dashed lines, respectively. Molar absorptivity is expressed per monomeric **G-1**. Arrows indicate the trend of intensity decrease during the heating.

Substantial changes also occur in the VCD spectra upon heating. The strong signal at 20 °C diminished rapidly and almost disappeared at 90 °C. Such intensity decrease (especially of the C=O modes) indicates a gradual loss of optical activity and is accompanied by weakening of the guanine carbonyl hydrogen bonds caused by elongation of the distances between the molecules and disruption of the supramolecular network. The products of the transition must be somehow less ordered showing weaker VCD signals than the aggregate in a gel state. From a macroscopic point of view, the hydrogel melts into the sol and the temperature of the gel–sol transition was found to be ~80 °C. Moreover, the lack of an isosbestic point in the temperature-dependent IR spectra suggests a multistate transition during the hydrogel melting and, therefore, indicates the formation of at least two different species in equilibrium (such as monomers, dimers, and other intermediates as detected by MS, see below).

ECD spectroscopy: To support our VCD data and better understand what happens with the optical activity of **G-1** during the self-association, we measured the temperature-dependent ECD spectra over a broad range of concentrations, from 0.04 to 20 mmol L^{-1}. The ECD spectra of the hydrogel obtained at the concentration of 20 mmol L^{-1} are presented in Figure 4. The strong positive band at 200 nm originates mainly from exciton coupling between guanine chromophores.[3,61–63] The sugars alone, D-ribose in our case, have the bands in the region below 190 nm, that partly overlap with the band at 200 nm from the aromatic chromophore, but their contribution is low at 200 nm. The ECD signals in the 250–320 nm region are generally determined by interaction between the guanine moieties. Therefore, the ECD

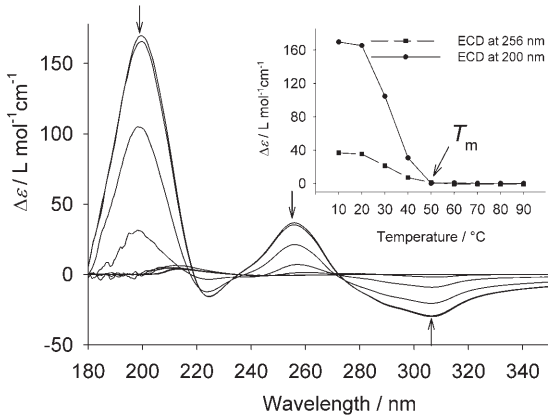

Figure 4. Gel melting experiment: ECD spectra of **G-1** at 20 mmol L^{-1} concentration in 0.5 mol L^{-1} deuterated sodium phosphate/D_2O buffer. Spectra were measured from 10 °C to 90 °C in 10 °C steps. Molar absorptivity is expressed per monomeric **G-1**. Arrows indicate the trend of intensity decrease during the heating. Inset: temperature dependence of the ECD signals at 200 nm (solid line) and 256 nm (dashed line) with indication of the gel melting temperature T_m.

bands presented in Figure 4 are primarily sensitive to the effect of self-assembly on the guanine part of the **G-1** molecule.

The spectrum at 10 °C shows a strong band at 200 nm (+) ($\Delta\varepsilon$ about 170 L mol^{-1} cm^{-1}!) and other bands at 225 (−), 256 (+), and 306 nm (−). Some of them, especially the negative and positive bands (positive couplet) between 220–270 nm, were found[3,22,64,65] to be diagnostic of the G-quartet and the stack formation; their signs are often correlated to the handedness of the columns, the positive couplet to a right-handed structure and the negative one to a left-handed structure.[22] While the ECD spectra of G-containing oligonucleotides may show a negative couplet, indicating a left-handed structure, the present spectra at low temperature are in a very good agreement with the spectra obtained on oligomers with a right-handed structure.[22] Therefore, this ECD finding supports our VCD data suggesting right-handed columnar stacks in the gel phase, rather than left-handed ones. When the sample is heated, the strong ECD signals are dramatically decreased and only new weak bands at 211 (+) and 245 nm (−) are observed at 90 °C. This indicates a transition of the columnar stacks $[(\mathbf{G\text{-}1})_4]_n$ to less ordered structures, primarily monomers of **G-1** that could be in equilibrium with dimers and other intermediates. This transition is accompanied by the melting of the gel at about 50 °C, as the plot describing the guanine ECD signal versus temperature shows. The value of melting temperature obtained is in very good agreement with the data obtained by test-tube-tilting method.[29]

Additional temperature-dependent ECD experiments were performed at lower concentration of **G-1** (4 mmol L^{-1}) in deuterated sodium phosphate/D_2O buffer and in pure D_2O (i.e., in presence and in absence of sodium cations, as templating cations may influence the structure of G-containing molecules[3]) to check for variation in spectral response under the different concentration conditions. The ECD spectrum of **G-1** at 4 mmol L^{-1} and at 10 °C in buffer (Figure 5) possesses the bands at 211 (+), 245 (−), 259 (+), and 306 nm (−), due all to the guanine chromophore coupling as shown in Figure 4. The ECD intensities are about 30 times lower in this case than observed at 20 mmol L^{-1} (Figure 4) and the positive band at 200 nm is missing. Nevertheless, the bands sensitive to columnar arrangement (couplet centered at about 250 nm consisting of negative and positive bands at ~240 and ~260 nm, respectively) of the **G-1** are apparent in the spectra at 10 and 20 °C.[3,22,64,65] Therefore, there is a coupling between the guanine bases at low temperatures, but not as strong as observed at 20 mmol L^{-1} because the ECD signal is about 28 times weaker. The gel–sol transition temperature decreases to about 30 °C in this case. Thus, the columnar structure is less stable and much sensitive to disruption by heating at this concentration. Actually, the ECD spectra measured at temperatures above 20 °C show the same pattern, the bands at 211 (+) and 245 nm (−). These indicate, in agreement with published ECD of GMP and G,[32] the presence of **G-1** in monomeric form after the self-assembly dissociation.

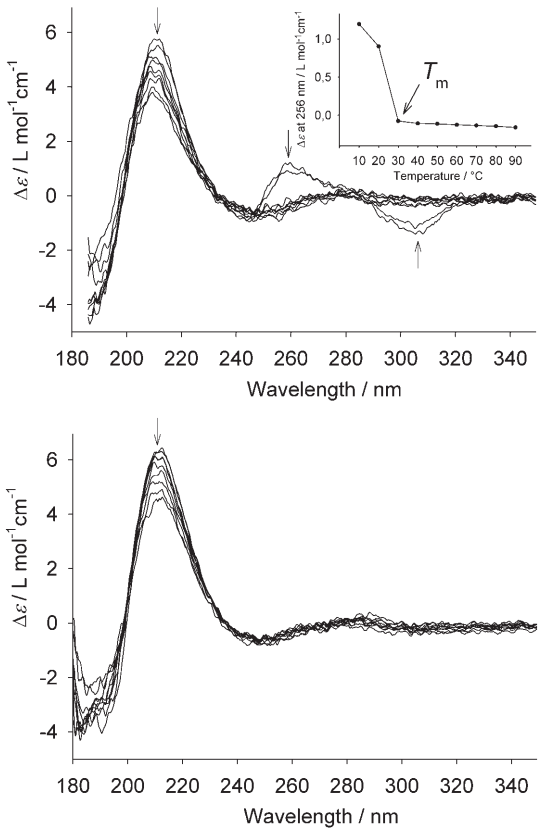

Figure 5. ECD spectra of **G-1** at 4 mmol L^{-1} concentration in 0.5 mol L^{-1} deuterated sodium phosphate/D_2O buffer (top) and in D_2O (bottom). Spectra were measured from 10 °C to 90 °C in 10 °C increments. Molar absorptivity is expressed per monomeric **G-1**. Arrows indicate the trend of intensity decrease during the heating. Inset: temperature dependence of the ECD signal at 256 nm.

In case of 4 mmol L^{-1} concentration in pure D_2O, that is, in absence of sodium cations, the G-stack "markers" at 245 (−), 259 (+), and 306 nm (−) are not observed anymore, indicating that there is weaker coupling between the guanine bases, as would be caused by formation and stacking of quartets, pointing to the presence of unordered species of **G-1** (i.e., monomers) at this concentration over the whole temperature range. The same is valid for even less concentrated samples, as the ECD spectra at 0.04 mmol L^{-1} indicate (Figure 6). The spectra are about the same in terms of spectral band shape (showing the bands at 211 (+) and 245 nm (−)) and intensities independently of the medium, buffer or pure D_2O. Thus, this concentration of **G-1** is too low to induce supramolecular assemblies and there is no sodium cation effect on the structure of **G-1** at such low concentration. In both solvents, our data show, in agreement with published results,[32] the presence of **G-1** monomers over the whole temperature range studied. A similar situation was observed in the IR spectra of **G-1** measured at low concentration in deuterated sodium phosphate/D_2O buffer and in pure D_2O (Figure 7). The positions and shapes of the ν(C=O) band at 1661 cm^{-1} and of the band at 1579 cm^{-1}, originating from δ(N−H) and aromatic ν(C=C) and ν(C=N),

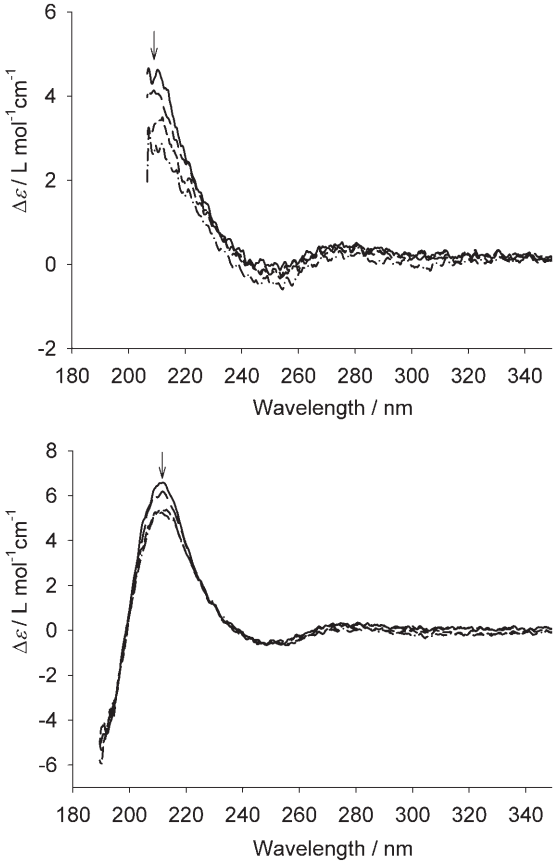

Figure 6. ECD spectra of **G-1** at 0.04 mmol L^{-1} concentration in 0.5 mol L^{-1} deuterated sodium phosphate/D_2O buffer (top) and in D_2O (bottom). Spectra were measured at 10, 40, 70, and 90 °C. Molar absorptivity is expressed per monomeric **G-1**. Arrows indicate the trend of intensity decrease during the heating.

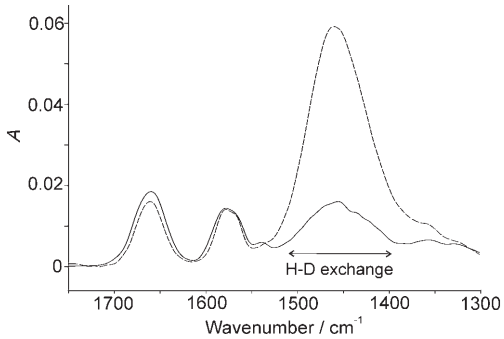

Figure 7. IR spectra of **G-1** in deuterated sodium phosphate/D_2O buffer (solid line) and in D_2O (dashed line); $c \sim 1$ mmol L^{-1}.

are about the same in the two media, indicating negligible effect of sodium cations on self-assembling of **G-1**. While the ECD spectroscopy data unambiguously show the presence of unordered forms of **G-1**, monomers, at 0.04 mmol L^{-1}, we used electrospray ionization mass spectrometry (ESI-MS) to more precisely specify the species that could be present in the sample at such level of **G-1** concentration. Firstly, it should be noted that MS does not give reliable information about the relative amounts of the different oligomers in solutions because it operates in a vapor phase. Furthermore, MS data do not give structural information, so that, for example, a tetramer observed in pure water may well not be of G-quartet type, although such structures may form in nonaqueous conditions.[66–68]

Mass spectrometry: The ESI-MS spectrum of **G-1** in pure water is shown in Figure 8. A peak at $m/z = 312.1$ indicates the presence of monomers (relative peak intensity ~22 % [**G-1**+H]$^+$). This species was also indicated by the ECD spectra as discussed above. Surprisingly, the most prevalent seems to be dimers $(\mathbf{G\text{-}1})_2$ (100 %, $m/z = 623.2$, $[(\mathbf{G\text{-}1})_2+H]^+$), in equilibrium with small amounts of trimers (~12 %, $m/z = 935.4$, $[(\mathbf{G\text{-}1})_3+H]^+$), and even more organized structures, tetramers (~6 %, $m/z = 1246.4$, $[(\mathbf{G\text{-}1})_4+H]^+$). Pentamers and higher associates were not observed. However, the ESI-MS experiments do not characterize the species in solution

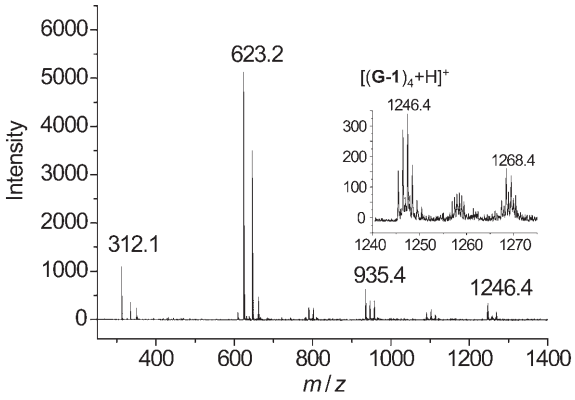

Figure 8. ESI-MS spectrum of **G-1** in pure water; $c \sim 0.2$ mmol L^{-1}.

but in the vapor phase. Therefore, the composition of the solutions may not correspond to that indicated by vapor phase measurement. Using buffer instead of water[29] (data not shown here), the ESI-MS spectrum shows a similar pattern. There is also a dominant peak of dimers (intensity 100%, m/z = 645.2, $[(\mathbf{G\text{-}1})_2+Na]^+$), but trimers are decreased in intensity to ~3% and tetramers are markedly higher (~28%, $m/z = 1267.4$, $[(\mathbf{G\text{-}1})_4+Na]^+$) than observed in pure water. Thus, as expected, sodium cations are required to stabilize the quartets $(\mathbf{G\text{-}1})_4$ and their ordered $[(\mathbf{G\text{-}1})_4]_n$ assemblies at higher concentrations. Then, the stacking of G-quartets can take place and is accompanied by gelation of the sample.

Finally, the MS results support our temperature-dependent IR spectra (Figure 3) for which the lack of an isosbestic point suggests a multistate transition when the hydrogel melts.

Conclusion

Investigation of the guanosine hydrazide **G-1** self-assembly by VCD and ECD provides new information on the nature of the supramolecular assemblies formed as well as on the effect of medium and temperature on these species. Taking into account all the results, **G-1** is present in the monomeric form in $[D_6]$DMSO, while the monomers are in equilibrium with other species such as dimers, trimers, and some other intermediates at 10 mmol L^{-1} concentration in sodium phosphate/D_2O buffer. If the **G-1** concentration is increased to 38 mmol L^{-1} in buffer, the sample becomes more viscous and eventually gives a stable hydrogel; the VCD and ECD intensities are then strongly enhanced. This might be attributed to the formation of highly organized supramolecular aggregate consisting of G-quartets, $(\mathbf{G\text{-}1})_4$ and their columnar stacks, $[(\mathbf{G\text{-}1})_4]_n$. The helical tubular polymers are structured as a stack of macrocyclic supramolecular quartets, $[(\mathbf{G\text{-}1})_4]_n$, containing sodium cations that probably occupy the central channel of the column and play an important role in the formation and stability of quadruplex structures. Disruption of the hydrogel takes place upon heating, as the $[(\mathbf{G\text{-}1})_4]_n$ assemblies dissociate into less ordered species, monomers in equilibrium with more or less important amounts of the **G-1** dimeric, trimeric, and other entities.

To obtain more information about the structures of particular species mentioned in this work, we have started ab initio DFT calculations of their IR and VCD spectra. Such calculations may serve to check our empirical observations presented here and help to understand the structure of the supramolecular species formed by **G-1**. It would also substantially extend the applicability of VCD, as a promising technique, to the field of supramolecular chemistry.

Acknowledgements

This work was supported by the Ministry of Education, Youth, and Sports of the Czech Republic, research grant No. MSM6046137307. We thank Mr. Vojtěch A. Borek (ICT Prague) for energy minimization and structure optimization, Mr. Jakub Nový and Dr. Stanislav Böhm (ICT Prague) for running ab initio calculations, and Dr. David Sýkora (ICT Prague) for helpful discussion of ESI-MS spectra.

[1] W. Guschlbauer, J.-F. Chantot, D. Thiele, *J. Biomol. Struct. Dyn.* **1990**, *8*, 491–511.
[2] J. T. Davis, *Angew. Chem.* **2004**, *116*, 684–716; *Angew. Chem. Int. Ed.* **2004**, *43*, 668–698.
[3] G. Gottarelli, G. P. Spada, A. Garbesi in *Comprehensive Supramolecular Chemistry, Vol. 9* (Eds.: J.-P. Sauvage, M. W. Hosseini), Pergamon, Oxford, **1996**, pp. 483–506.
[4] G. Gottarelli, G. P. Spada, *Chem. Rec.* **2004**, *4*, 39–49.
[5] J. Deng, Y. Xiong, M. Sundaralingam, *Proc. Natl. Acad. Sci. USA* **2001**, *98*, 13665–13670.
[6] S. L. Forman, J. C. Fettinger, S. Pieraccini, G. Gottarelli, J. T. Davis, *J. Am. Chem. Soc.* **2000**, *122*, 4060–4067.
[7] C. H. Kang, X. Zhang, R. Ratliff, R. Moyzis, A. Rich, *Nature* **1992**, *356*, 126–131.
[8] G. Laughlan, A. I. H. Murchie, D. G. Norman, M. H. Moore, P. C. E. Moody, D. M. J. Lilley, B. Luisi, *Science* **1994**, *265*, 520–524.
[9] K. Phillips, Z. Dauter, A. I. H. Murchie, D. M. J. Lilley, B. Luisi, *J. Mol. Biol.* **1997**, *273*, 171–182.
[10] X. Shi, K. M. Mullaugh, J. C. Fettinger, Y. Jiang, S. A. Hofstadler, J. T. Davis, *J. Am. Chem. Soc.* **2003**, *125*, 10830–10841.
[11] T. Sunami, J. Kondo, T. Kobuna, I. Hirao, K. Watanabe, K. I. Miura, A. Takenaka, *Nucleic Acids Res.* **2002**, *30*, 5253–5260.
[12] K. Fukushima, H. Iwahashi, *Chem. Commun.* **2000**, *11*, 895–896.
[13] G. Gottarelli, E. Mezzina, G. P. Spada, F. Carsughi, G. Di Nicola, P. Mariani, A. Sabatucci, S. Bonazzi, *Helv. Chim. Acta* **1996**, *79*, 220–234.
[14] T. J. Pinnavaia, C. L. Marshall, C. M. Mettler, C. L. Fisk, H. T. Miles, E. D. Becker, *J. Am. Chem. Soc.* **1978**, *100*, 3625–3627.
[15] A. Wong, R. Ida, L. Spindler, G. Wu, *J. Am. Chem. Soc.* **2005**, *127*, 6990–6998.
[16] J. T. Davis, S. K. Tirumala, A. L. Marlow, *J. Am. Chem. Soc.* **1997**, *119*, 5271–5272.
[17] T. Giorgi, F. Grepioni, I. Manet, P. Mariani, S. Maseiro, E. Mezzina, S. Pieraccini, L. Saturni, G. P. Spada, G. Gottarelli, *Chem. Eur. J.* **2002**, *8*, 2143–2152.
[18] E. Mezzina, P. Mariani, R. Itri, S. Masiero, S. Pieraccini, G. P. Spada, F. Spinozzi, J. T. Davis, G. Gottarelli, *Chem. Eur. J.* **2001**, *7*, 388–395.
[19] J.-M. Lehn, *Science* **2002**, *295*, 2400–2403.
[20] J.-M. Lehn, *Proc. Natl. Acad. Sci. USA* **2002**, *99*, 4763–4768.
[21] M. M. Cai, X. D. Shi, V. Sidorov, D. Fabris, Y. Lam, J. T. Davis, *Tetrahedron* **2002**, *58*, 661–671.
[22] G. Gottarelli, G. P. Spada in *Circular Dichroism: Principles and Applications*, 2nd ed. (Eds.: N. Berova, K. Nakanishi, R. W. Woody), Wiley, New York, **2000**, pp. 547–561.
[23] I. Haq, J. Ladbury, *J. Mol. Recognit.* **2000**, *13*, 188–197.
[24] F. B. Howard, J. Frazier, T. Miles, *Biopolymers* **1977**, *16*, 791–809.
[25] D. Rhodes, R. Giraldo, *Curr. Opin. Struct. Biol.* **1995**, *5*, 311–322.
[26] S. Neidle, M. A. Read, *Biopolymers* **2000**, *5*, 195–208.
[27] M. A. Read, A. A. Wood, J. R. Harrison, S. M. Gaowan, L. R. Kelland, H. S. Dosanjh, S. Neidle, *J. Med. Chem.* **1999**, *42*, 4538–4546.
[28] D. E. Gilbert, J. Feigon, *Curr. Opin. Struct. Biol.* **1999**, *9*, 305–314.
[29] N. Sreenivasachary, J. M. Lehn, *Proc. Natl. Acad. Sci. USA* **2005**, *102*, 5938–5943.
[30] W. C. Johnson in *Circular Dichroism: Principles and Applications*, 2nd ed. (Eds.: N. Berova, K. Nakanishi, R. W. Woody), Wiley, New York, **2000**, pp. 703–718.
[31] *Circular Dichroism: Principles and Applications*, 2nd ed. (Eds.: N. Berova, K. Nakanishi, R. W. Woody), Wiley, New York **2000**.

[32] C. A. Sprecher, W. C. Johnson, Jr., *Biopolymers* **1977**, *16*, 2243–2264.
[33] T. Giorgi, S. Lena, P. Mariani, M. A. Cremonini, S. Masiero, S. Pieraccini, J. P. Rabe, P. Samori, G. P. Spada, G. Gottarelli, *J. Am. Chem. Soc.* **2003**, *125*, 14741–14749.
[34] P. J. Stephens, *J. Phys. Chem.* **1985**, *89*, 748–752.
[35] L. A. Nafie, T. B. Freedman in *Circular Dichroism: Principles and Applications*, 2nd ed. (Eds.: N. Berova, K. Nakanishi, R. W. Woody), Wiley, New York, **2000**, pp. 97–132.
[36] T. A. Keiderling in *Circular Dichroism: Principles and Applications*, 2nd ed. (Eds.: N. Berova, K. Nakanishi, R. W. Woody), Wiley, New York, **2000**, pp. 621–666.
[37] P. L. Polavarapu, Ch. Zhao, *Fresenius J. Anal. Chem.* **2000**, *366*, 727–734.
[38] M. Urbanová, V. Setnička, V. Král, K. Volka, *Biopolymers* **2001**, *60*, 307–316.
[39] P. Bouř, K. Záruba, M. Urbanová, V. Setnička, P. Matějka, Z. Fiedler, K. Volka, *Chirality* **2000**, *12*, 191–198.
[40] A. Synytsya, M. Urbanová, V. Setnička, M. Tkadlecová, J. Havlíček, I. Raich, P. Matějka, A. Synytsya, J. Èopíková, K. Volka, *Carbohydr. Res.* **2004**, *339*, 2391–2405.
[41] Z. Tománková, V. Setnička, M. Urbanová, P. Matějka, V. Král, K. Volka, P. Bouř, *J. Org. Chem.* **2004**, *69*, 26–32.
[42] J. Nový, M. Urbanová, K. Volka, *J. Mol. Struct.* **2005**, *748*, 17–25.
[43] L. Palivec, M. Urbanová, K. Volka, *J. Pept. Sci.* **2005**, *11*, 536–545.
[44] M. Urbanová, V. Setnička, F. J. Devlin, P. J. Stephens, *J. Am. Chem. Soc.* **2005**, *127*, 6700–6711.
[45] V. Setnička, M. Urbanová, S. Pataridis, V. Král, K. Volka, *Tetrahedron: Asymmetry* **2002**, *13*, 2661–2666.
[46] V. Král, S. Pataridis, V. Setnička, K. Záruba, M. Urbanová, K. Volka, *Tetrahedron* **2005**, *61*, 5499–5506.
[47] M. Urbanová, V. Setnička, K. Volka, *Chirality* **2000**, *12*, 199–203.
[48] M. Banyay, M. Sarkar, A. Gräslund, *Biophys. J.* **2003**, *104*, 477–488.
[49] L. Wang, L. Yang, T. A. Keiderling, *Biophys. J.* **1994**, *67*, 2460–2467.
[50] V. V. Andruschenko, J. H. Van de Sande, H. Wieser, S. V. Kornilova, Y. P. Blagoi, *J. Biomol. Struct. Dyn.* **1999**, *17*, 545–560.
[51] M. Gulotta, D. J. Goss, M. Diem, *Biopolymers* **1989**, *28*, 2047–2058.
[52] L. Wang, T. A. Keiderling, *Biochemistry* **1992**, *31*, 10265–10271.
[53] V. V. Andruschenko, J. H. Van de Sande, H. Wieser, *Biopolymers* **2003**, *72*, 374–390.
[54] M. Meyer, T. Steinke, M. Brandl, J. Suhnel, *J. Comput. Chem.* **2001**, *22*, 109–124.
[55] J. Gu, J. Leszczynski, *J. Phys. Chem. A* **2000**, *104*, 6308–6313.
[56] J. Gu, J. Leszczynski, *J. Phys. Chem. A* **2002**, *106*, 529–532.
[57] A. Calzorazi, R. Di Felice, E. Molinari, A. Garbesi, *Appl. Phys. Lett.* **2002**, *80*, 3331–3333.
[58] X. Shi, J. C. Fettinger, J. T. Davis, *J. Am. Chem. Soc.* **2001**, *123*, 6738–6739.
[59] X. Shi, J. C. Fettinger, J. T. Davis, *Angew. Chem.* **2001**, *113*, 2909–2913; *Angew. Chem. Int. Ed.* **2001**, *40*, 2827–2831.
[60] S. Neidle, in *Nucleic Acid Structure and Recognition*, Oxford University Press, Oxford, **2002**, p. 77.
[61] D. M. Gray in *Circular Dichroism: Principles and Applications*, 2nd ed. (Eds.: N. Berova, K. Nakanishi, R. W. Woody), Wiley, New York, **2000**, pp. 769–796.
[62] A. Koslowski, N. Sreerama, R. W. Woody in *Circular Dichroism: Principles and Applications*, 2nd ed. (Eds.: N. Berova, K. Nakanishi, R. W. Woody), Wiley, New York, **2000**, pp. 55–95.
[63] J. C. Maurizot in *Circular Dichroism: Principles and Applications*, 2nd ed. (Eds.: N. Berova, K. Nakanishi, R. W. Woody), Wiley, New York, **2000**, pp. 719–739.
[64] G. Gottarelli, P. Palmieri, G. P. Spada, F. Carsughi, G. Di Nicola, P. Mariani, A. Sabatucci, S. Bonazzi, *Gazz. Chim. Ital.* **1990**, *120*, 101–107.
[65] J. Kypr, M. Fialová, J. Chládková, M. Tůmová, M. Vorlíčková, *Eur. Biophys. J.* **2001**, *30*, 555–558.
[66] The formation of supramolecular quartet structures in absence of sodium ions has been reported for guanosine derivatives in organic medium[67] and for guanine itself on a gold surface.[68]
[67] J. L. Sessler, M. Sathiosatham, K. Doerr, V. Lynch, K. H. Abboud, *Angew. Chem.* **2000**, *112*, 1356–1369; *Angew. Chem. Int. Ed.* **2000**, *39*, 1300–1303.
[68] R. Otero, M. Schöck, L. M. Molina, E. Laegsgaard, I. Stensgaard, B. Hammer, F. Besenbacher, Angew. Chem. **2000**, *117*, 2310–2315; *Angew. Chem. Int. Ed.* **2005**, *44*, 2270–2275.

Received: August 10, 2005
Revised: June 26, 2006
Published online: September 19, 2006

